Article:
Koshuriyan, Zamir, Goldstein, Marvin and Fagan, Amy (2011) Enthalpy flux/momentum flux coupling in the acoustic spectrum of heated jets. AIAA Journal. pp. 2522-2531. ISSN 0001-1452

https://doi.org/10.2514/1.J051076

Enthalpy flux—momentum flux coupling in the acoustic spectrum of heated jets

M. Z. Afsar[1*], M. E. Goldstein[2] and A. Fagan[2]

[1]Ohio Aerospace Institute, 22800 Cedar Point Road, Cleveland, OH 44142.

[2]National Aeronautics and Space Administration, Glenn Research Center, Cleveland, OH 44135, USA.

[*] Email address: mohammed.afsar@cantab.net

Abstract[†]

Exhaust flows from aircraft engines operate at higher temperatures than the free stream. Accurate predictions of jet noise in heated flows is therefore of considerable interest. In this paper, we develop a self-consistent jet noise model in heated flows using the generalized acoustic analogy derived in reference [1]. We show that the acoustic spectrum can be written as the sum of three terms: the momentum flux auto-covariance term, the enthalpy flux—momentum flux covariance (or the coupling term) and the enthalpy flux auto-covariance. By extending the axi-symmetric model of the Reynolds stress auto-covariance developed and verified in Afsar *et al* [2], to heated jet turbulence, we reduce the number of independent components in the acoustic spectrum to 11 terms. We focus on the structure of the coupling term, and use recent Rayleigh scattering measurements in heated flows taken at NASA Glenn to show that it becomes increasingly important as the acoustic Mach number increases. That is, it can provide either, enhancement, or cancellation to the acoustic spectrum depending on the acoustic Mach number and the position of the observation point. This behavior can help explain why heating reduces the overall sound pressure level (OASPL) at all observation angles in supersonic jets.

† Presented at the 49th Aerospace Sciences Meeting in Orlando, Florida, 4th – 7th January 2011.

Nomenclature

$A_{\mu l}$	=	amplitude function
$A_{1,2,3...}$	=	scalar field
c	=	sound speed
c_∞	=	ambient sound speed
D_{jet}	=	nozzle diameter
$g^a_{\mu l}$	=	adjoint vector Green's function
h	=	enthalpy
$H_{\mu j,\nu l}$	=	generalized Reynolds stress auto-covariance spectrum
I_ω	=	acoustic spectrum
$\underline{k}$	=	wave number vector
$\underline{k}_\perp$	=	transverse wave number vector
L	=	streamwise length scale
M	=	acoustic Mach number
p	=	pressure
$R_{\mu j,\nu l}$	=	generalized Reynolds stress auto-covariance tensor
S	=	eikonal
(τ, t)	=	time
T	=	averaging time
U_c	=	convection velocity
V_∞	=	source volume
v_i	=	velocity vector
v_4	=	generalized enthalpy fluctuation

$\underline{x}$ = observer location

$\underline{y}$ = source location

γ = specific heat ratio

$\gamma_{\nu j}$ = propagator

$\Gamma_{\nu j}$ = Fourier-transformed propagator

δ_{ij} = unit tensor

$\underline{\eta}$ = separation vector

$\underline{\eta}_{\perp}$ = transverse separation vector

$\Phi_{\mu j,\nu l}$ = space-time spectrum of the generalized Reynolds stress auto-covariance tensor

ρ = density

θ = polar angle measured from jet axis

τ_0 = time delay

ω = radian frequency

$|...|$ = absolute value

Subscripts

(i, j, k, l) = tensor suffixes $= 1, 2, 3$

$\perp$ = transverse component

(μ, ν) = tensor suffixes $= 1, 2, 3, 4$

Superscripts

a = adjoint

$\bar{\bullet}$	=	time average
$'$	=	fluctuating quantity
$\tilde{\bullet}$	=	Favre average
$*$	=	complex conjugate

1. INTRODUCTION

Since aircraft engine exhaust streams tend to be quite hot, there is an ongoing effort to develop mathematical models for predicting the aero-acoustics of heated jets across a Mach number range extending from subsonic to low supersonic flow ([3], [4], [5]). While accounting for "temperature effects" in jet noise predictions is not new (Lush & Fischer [6], Morfey *et al* [7] and Lilley [8]), recent advances in modeling cold jet acoustics (see reference [9]) provide a theoretical basis for developing a much more rigorous theory of heated jet flows. One purpose of this paper is to lay the foundation for a theory of this type, but the main focus will be on a phenomenon that has been previously neglected in jet noise modeling: namely the influence the "enthalpy flux—momentum flux" noise source coupling term has on the aero-acoustics of heated flows. We examine the effect of this coupling term on the overall acoustic spectrum and show that it becomes increasingly important for near transonic and supersonic heated flows and is likely to become negative at supersonic speeds. This particular result may help explain why experiments (Tanna [10], Harper-Bourne [11], Tester & Morfey [12] and Viswanathan [13]) and computational studies (Andersson [14], Moore *et al* [15] and Bodony & Lele [16]) show that heating reduces the overall sound pressure level (OASPL) at supersonic speed.

Acoustic analogy based models are able to produce reasonably good predictions of the observed acoustic spectrum in cold flows; see [9]. Reference [9] used the formalism developed in [1] and certain statistical assumptions about the turbulence to predict cold jet acoustic spectra that were in reasonable agreement with recent jet noise measurements. But the analysis was based on certain assumptions about the Reynolds stress auto-covariance that were more restrictive than necessary (see Afsar [17] for further analysis of these assumptions). Since our goal is to put the present theory on as firm a foundation as possible,

we first eliminate the unnecessary assumptions used in reference [9] before extending it to heated flows. The resulting formula for the acoustic spectrum is the sum of three terms that depend on different components of the generalized turbulence auto-covariance tensor introduced in [9]. The first of these involves the momentum flux auto-covariance; the second, the co-variance between the enthalpy flux and momentum flux (or the coupling term); and the third involves the enthalpy flux auto-covariance.

As indicated above, the main focus of this paper is on the coupling term, which has not been considered in previous jet noise models. The acoustic Mach number is assumed to be less than 1.5 in order to ensure that the convection Mach number is always subsonic. Recent Rayleigh scattering data taken at NASA Glenn is used to show that this term becomes increasingly important as the Mach number increases while the analysis shows that its sign can become negative at supersonic speeds. This term can, therefore, reduce the radiated sound field. The Rayleigh scattering data is also used to show how the coupling term becomes increasingly important at supersonic speeds. This result is the most novel contribution of the paper.

A large body of acoustic data has been obtained for heated jets in the decades following Lighthill's [18] proposal of the acoustic analogy (e.g. [19], [20], [6], [21], [22], [23], [24], [25], [26], [10], [7] and [27]). More recent experiments were designed to check the accuracy of earlier studies and to extend their applicability to a greater parameter range; (e.g. [28], [29], [30], [31], [32], [33], [34], [35], [36], [11], [37], [38], [39], [40], [41] and [42]).

It is still challenging to measure turbulence correlations of the type needed for jet noise modeling (see Karabasov *et al* [43])—especially when the correlation tensor involves transverse separations (Viswanathan [44], [45] and Mielke *et al* [40]). Moreover, there are almost no measurements of the enthalpy—velocity correlations that appear in the acoustic

formulas for heated flows. However it is now becoming less expensive to use large eddy simulations (LES) and direct numerical simulations (DNS) to calculate the turbulence properties of heated flows (e.g., Bogey & Bailly [46], Bogey *et al* [47], Gerolymos [48], Lew *et al* [49], Moore *et al* [15], Bodony & Lele [16] and Bodony [50]) and there is some hope that these results can eventually be used to develop the turbulence auto-covariance models needed for predict the sound from hot jets.

Tester & Morfey [12] and Lilley [8] were among the first to argue that it is necessary to include enthalpy fluctuation "source terms" in order to obtain more realistic predictions of the acoustic measurements. More recent support for this idea is also given by Harper-Bourne [11]. Further evidence for the importance of this term is provided by recent LES-based jet noise predictions (see Andersson [14], Lew *et al* [49]; Bodony & Lele [16] and Bodony [50]). These calculations show that noise predictions based on Lighthill's analogy is much more accurate in heated flows when the pressure-density term --- sometimes referred to as the "entropy term"--- is included. For example, Andersson [14] showed that the large angle OASPL (figure 7.74) can be significantly over predicted when only the momentum flux source is present. Although Andersson [14] did not explicitly show that the pressure-density term would produce better predictions at large angles, Lew *et al* [49] did confirm this for a heated jet at a Mach number of 0.9 (see their figure 11). Bodony & Lele [16] showed that the cancellation between the momentum flux and pressure-density terms is significant in heated flows, and especially at small observation angles.

Most of these computational studies were interpreted in terms of Lighthill's formulation– presumably because of its simplicity. But there are technical difficulties in using it as a starting point for mathematical modeling in heated flows—mainly because the pressure density term that appears in the Lighthill source function contains both isentropic

and non-isentropic components with the latter being proportional to viscous and heat conduction effects which are believed to be negligible at the high Reynolds numbers of interest in jet noise problems. The present paper extends the axi-symmetry model of Afsar *et al* [2] to obtain a self consistent model for the enthalpy coupling term and the enthalpy flux auto-covariance term in the formula for the acoustic spectrum and uses the result along with data from recent measurements of the correlations function amplitudes taken at the NASA Glenn Research Center to obtain a better theoretical understanding of the acoustic spectrum for heated jets. But no attempt is made to make quantitative predictions of the radiated sound since the appropriate space-time data is not yet available for the enthalpy correlation functions. The coupling term, which has not been considered in previous studies, is shown to play an important role at high acoustic Mach numbers. We show that this term can become negative when the local mean flow velocity is supersonic (with the source convection speed still subsonic) and the observation point is close to the jet axis. This phenomenon may, therefore, provide a possible basis for new noise reduction methods, particularly for the peak noise at small angles to the jet axis.

The remainder of the paper is organized as follows. The basic formalism is summarized in Section 2. The statistical axi-symmetry model and the WKBJ approximation are used to simplify the formula for the acoustic spectrum formula in Section 3. The statistical axi-symmetry model is used to in section 4 to decompose the auto-covariance tensor into three components. Section 5 uses these results and Recent Rayleigh scattering data to explain the gross features of the acoustic spectrum in heated jets across a range of Mach numbers and temperature ratios.

2. THE FUNDAMENTAL EQUATION

The acoustic spectrum,

$$I_\omega(\underline{x}) = \int_{-\infty}^{+\infty} e^{i\omega\tau_0}\overline{p^2}(\underline{x},\tau_0)\,d\tau_0 \tag{1}$$

at the observation point $\underline{x}$, i.e. the Fourier transform of the far-field pressure auto-covariance

$$\overline{p^2}(\underline{x},\tau_0) = \frac{1}{2T}\int_{-T}^{+T} p(\underline{x},t)p(\underline{x},t+\tau_0)\,dt \tag{2}$$

can be expressed in terms of $I_\omega(\underline{x} \mid \underline{y})$, the acoustic spectrum at $\underline{x}$, due to a unit volume of turbulence at $\underline{y}$, by the equation:

$$I_\omega(\underline{x}) = \int_{V_\infty(\underline{y})} I_\omega(\underline{x} \mid \underline{y})\,d\underline{y}, \tag{3}$$

where $V_\infty(\underline{y})$ denotes integration over all space with respect to $\underline{y}$. Reference [9] shows that this latter quantity is given by

$$I_\omega(\underline{x} \mid \underline{y}) = (2\pi)^2\Gamma_{\nu j}(\underline{x} \mid \underline{y};\omega)\int_{V_\infty(\underline{\eta})} \Gamma^*_{\mu l}(\underline{x} \mid \underline{y}+\underline{\eta};\omega)\mathcal{H}_{\nu j,\mu l}(\underline{y},\underline{\eta},\omega)\,d\underline{\eta}, \tag{4}$$

where the asterisks denote complex conjugate, Greek suffixes range from 1 to 4, and Latin suffixes from 1 to 3. The second rank tensor defined by,

$$\Gamma_{\nu j}(\underline{x} \mid \underline{y};\omega) = \frac{1}{2\pi}\int_{-\infty}^{+\infty} e^{i\omega(t-\tau)}\gamma_{\nu j}(\underline{x} \mid \underline{y},t-\tau)\,d(t-\tau), \tag{5}$$

is the Fourier transform of a "propagator"

$$\gamma_{\nu j}(\underline{x},t \mid \underline{y},\tau) = \frac{\partial g^a_{\nu 4}(\underline{x},t \mid \underline{y},\tau)}{\partial y_j} - (\gamma-1)\delta_{\nu k}\frac{\partial \tilde{v}_k}{\partial y_j}g^a_{44}(\underline{x},t \mid \underline{y},\tau), \tag{6}$$

that depends on the adjoint vector Green's function $g^a_{\mu\nu}(\underline{y},\tau \mid \underline{x},t)$, determined by equations (4.8) and (4.11) of reference [9], which shows that the Green's function and, therefore, $\gamma_{\nu j}(\underline{x},t \mid \underline{y},\tau)$ can be calculated once the mean flow is known.

The rank four tensor, $\mathcal{H}_{\nu j,\mu l}(\underline{y},\underline{\eta},\omega)$ is related to the generalized fluctuating stress tensor

$$R_{\nu j,\mu l}(\underline{y},\underline{\eta},\tau_0) = \frac{1}{2T}\int_{-T}^{+T}\left[\rho v'_\nu v'_j - \overline{\rho v'_\nu v'_j}\right](\underline{y},\tau)\left[\rho v'_\mu v'_l - \overline{\rho v'_\mu v'_l}\right](\underline{y}+\underline{\eta},\tau+\tau_0)\,d\tau, \tag{7}$$

by the simple linear transformation,

$$\mathcal{H}_{\nu j,\mu l} = \epsilon_{\nu j,\sigma m} H_{\sigma m,\lambda n}\epsilon_{\mu l,\lambda n}, \tag{8}$$

where

$$H_{\nu j,\mu l}(\underline{y},\underline{\eta},\omega) = \frac{1}{2\pi}\int_{-\infty}^{+\infty} e^{-i\omega\tau_0} R_{\nu j,\mu l}(\underline{y},\underline{\eta},\tau_0)\,d\tau_0, \tag{9}$$

$\tilde{v}_k$ denotes the Favre averaged mean flow velocity, the overbar denotes the time average and,

$$\epsilon_{\nu j,\sigma m} = \left(\delta_{\nu\sigma}\delta_{jm} - \frac{\gamma-1}{2}\delta_{\nu j}\delta_{\sigma m}\right). \tag{10}$$

$v'_\mu(\underline{y},\tau) \equiv v_\mu(\underline{y},\tau) - \tilde{v}_\mu(\underline{y})$ denotes a four dimensional velocity fluctuation, with the fourth component defined by

$$v'_4(\underline{y},\tau) = (\gamma-1)\left[h' + \frac{1}{2}v'^2\right](\underline{y},\tau) = \left(c^2\right)' + \frac{\gamma-1}{2}v'^2 \tag{11}$$

where h' denotes the enthalpy fluctuation, $(c^2)'$ denotes the fluctuation in the squared sound speed and $v'_4/(\gamma-1)$ denotes the moving frame stagnation enthalpy fluctuation. The dimensionless ratio, $v'_4/U_{\text{jet}}v'_j$, which determines the relative importance of the fourth component of v'_μ to v'_i, where U_{jet} denotes a characteristic jet velocity, must scale as

$O(\sqrt{v'^2}/U_{\text{jet}})$ for unheated jets when the Mach number is $O(1)$ (see, Lilley [51] and Morfey, Szewczyk & Tester [52]) because c'^2 is expected to be $O(\sqrt{v'^2})^2$ in this case. The enthalpy component of v'_μ should, therefore, be small for cold jets and can be set to zero in $R_{\nu j,\mu l}(\underline{y},\underline{\eta},\tau_0)$, which will equal zero whenever $(\mu,\nu)=4$.

Equation (7) shows that the generalized Reynolds stress auto-covariance tensor $R_{\nu j,\mu l}(\underline{y},\underline{\eta},\tau_0)$ possesses pair symmetry in the suffixes (ν,j) when $\nu=(1,2,3)$ and in the suffixes (μ,l) when $\mu=(1,2,3)$. It, therefore, follows from equations (8) - (10) that the transformed tensor $\mathcal{H}_{\nu j,\mu l}$ also has this property. Then since this symmetry does not exist when the corresponding Greek suffix is equal to 4, it makes sense to re-write equation (4) as

$$
\begin{aligned}
I_\omega(\underline{x}\mid\underline{y}) = (2\pi)^2\Gamma_{ij}(\underline{x}\mid\underline{y};\omega)\int\limits_{V_\infty(\underline{\eta})}\Gamma^*_{kl}(\underline{x}\mid\underline{y}+\underline{\eta};\omega)\mathcal{H}_{ij,kl}(\underline{y},\underline{\eta},\omega)\,d\underline{\eta}\\
+\ (2\pi)^2\Gamma_{ij}(\underline{x}\mid\underline{y};\omega)\int\limits_{V_\infty(\underline{\eta})}\Gamma^*_{4l}(\underline{x}\mid\underline{y}+\underline{\eta};\omega)\mathcal{H}_{ij,4l}(\underline{y},\underline{\eta},\omega)\,d\underline{\eta}\\
+\ (2\pi)^2\Gamma_{4j}(\underline{x}\mid\underline{y};\omega)\int\limits_{V_\infty(\underline{\eta})}\Gamma^*_{kl}(\underline{x}\mid\underline{y}+\underline{\eta};\omega)\mathcal{H}_{4j,kl}(\underline{y},\underline{\eta},\omega)\,d\underline{\eta}\\
+\ (2\pi)^2\Gamma_{4j}(\underline{x}\mid\underline{y};\omega)\int\limits_{V_\infty(\underline{\eta})}\Gamma^*_{4l}(\underline{x}\mid\underline{y}+\underline{\eta};\omega)\mathcal{H}_{4j,4l}(\underline{y},\underline{\eta},\omega)\,d\underline{\eta}
\end{aligned}
\tag{12}
$$

But since

$$
\begin{aligned}
R_{\nu j,\mu l}(\underline{y},\underline{\eta},\tau_0) &= \frac{1}{2T}\int\limits_{-T}^{+T}\left[\rho v'_\nu v'_j-\overline{\rho v'_\nu v'_j}\right](\underline{y},\tau)\left[\rho v'_\mu v'_l-\overline{\rho v'_\mu v'_l}\right](\underline{y}+\underline{\eta},\tau+\tau_0)\,d\tau,\\
&= R_{\mu l,\nu j}(\underline{y}+\underline{\eta},-\underline{\eta},-\tau_0)
\end{aligned}
\tag{13}
$$

it follows from equations (8) - (10) that

$$\mathcal{H}^*_{\nu j,\mu l}(\underline{y},\underline{\eta},\omega) = \mathcal{H}_{\mu l,\nu j}(\underline{y}+\underline{\eta},-\underline{\eta},\omega) \tag{14}$$

The integration variables and index names can, therefore, be changed in the formula for the contribution of the second term in equation (12) to the integral $I_\omega(\underline{x}) = \int\limits_{V_\infty(\underline{y})} I_\omega(\underline{x} \mid \underline{y})\, d\underline{y}$ to show that the third term makes the same contribution to this integral as the complex conjugate of the second term, which means that the acoustic spectrum $I_\omega(\underline{x} \mid \underline{y})$ due to a unit volume of turbulence at $\underline{y}$, can also be expressed as the sum

$$\frac{I_\omega(\underline{x} \mid \underline{y})}{(2\pi)^2} = I^{[1]}_\omega\,(\underline{x} \mid \underline{y}) + I^{[2]}_\omega\,(\underline{x} \mid \underline{y}) + I^{[3]}_\omega\,(\underline{x} \mid \underline{y}) \tag{15}$$

of the following three terms

(i). The momentum flux auto-covariance term:

$$I^{[1]}_\omega\,(\underline{x} \mid \underline{y}) = G_{ij}(\underline{x} \mid \underline{y};\omega) \int\limits_{V_\infty(\underline{\eta})} G^*_{kl}(\underline{x} \mid \underline{y}+\underline{\eta};\omega)\mathcal{H}_{ij,kl}(\underline{y},\underline{\eta},\omega)\, d\underline{\eta} \tag{15a}$$

(ii). The enthalpy flux – momentum flux covariance (or, the coupling term):

$$I^{[2]}_\omega\,(\underline{x} \mid \underline{y}) = 2\mathrm{Re}\left\{ \Gamma_{4j}(\underline{x} \mid \underline{y};\omega) \int\limits_{V_\infty(\underline{\eta})} G^*_{kl}(\underline{x} \mid \underline{y}+\underline{\eta};\omega)\mathcal{H}_{4j,kl}(\underline{y},\underline{\eta},\omega)\, d\underline{\eta} \right\} \tag{15b}$$

and (iii) The enthalpy flux auto-covariance term:

$$I^{[3]}_\omega\,(\underline{x} \mid \underline{y}) = \Gamma_{4j}(\underline{x} \mid \underline{y};\omega) \int\limits_{V_\infty(\underline{\eta})} \Gamma^*_{4l}(\underline{x} \mid \underline{y}+\underline{\eta};\omega)\mathcal{H}_{4j,4l}(\underline{y},\underline{\eta},\omega)\, d\underline{\eta} \tag{15c}$$

where Re denotes the real part and we have introduced the symmetric tensor $G_{ij} = (\Gamma_{ij} + \Gamma_{ji})/2$ since $\mathcal{H}_{ij,kl}$ has pair symmetries in its first and second pairs of suffixes

and $\mathcal{H}_{4j,kl}$ possesses one pair symmetry in its last pair. Notice that the enthalpy flux – momentum flux coupling term involves the covariance of the enthalpy flux at (at location, $\underline{y}$) with the momentum flux (at location, $\underline{y}+\underline{\eta}$) while the enthalpy flux term involves the auto-covariance of the enthalpy flux itself.

3. APPROXIMATIONS

3.1. Kinematic approximations 1 and 2

The generalized Reynolds stress auto-covariance tensor $R_{\nu j,\mu l}$ that enters the acoustic spectrum through equations (8) & (9) has 63 independent components. It is, therefore necessary, to introduce some approximations to reduce this number to a reasonable value. This was accomplished for cold jets in Afsar *et al* [2] by introducing a statistical axi-symmetry model for the Reynolds stress auto-covariance tensor $R_{ij,kl}$ or equivalently its Fourier transform $H_{ij,kl}(\underline{y},\underline{\eta},\omega)$, which was verified against turbulence data from the PIV experiments of Pokora & McGuirk [53] and a large eddy simulation (LES) of a cold jet flow. Appendix A contains a shorter version of the verification given in Afsar *et al* [2]. Since the results show that the model is fairly accurate it seems appropriate to extend it to the generalized auto-covariance tensor $R_{\nu j,\mu l}$ (or equivalently its Fourier transform $H_{\nu j,\mu l}$) by introducing the following two basic assumptions:

Assumption 1: $H_{\nu j,\mu l}(\underline{y},\underline{\eta},\omega)$ depends upon $\underline{\eta}_{\perp}$ only through its magnitude, $|\underline{\eta}_{\perp}|$ or in symbolic form

$$H_{\nu j,\mu l}(\underline{y},\eta_1,\underline{\eta}_{\perp},\omega) \approx H_{\nu j,\mu l}(\underline{y},\eta_1,|\underline{\eta}_{\perp}|,\omega) \tag{16}$$

However, as noted in Afsar *et al* [2] the Harper-Bourne [54] and Pokora & McGuirk [53] experiments suggest turbulence in the round jet flow is more or less axi-symmetric. This is demonstrated by figure (10) of Pokora & McGuirk [53] which shows that the axial correlation length of $R_{11,11}$ (figure 10b) is significantly greater than the correlation lengths in either of the transverse directions (see figures 10d and 10f in Pokora & McGuirk [53]). Hence, it is reasonable to suppose $R_{\nu j,\mu l}(\underline{y},\underline{\eta},\tau_0)$ is itself an axi-symmetric tensor, which means that the 4th, 3rd and 2nd rank tensors $R_{ij,kl}$, $R_{4j,kl}$ and $R_{4j,4l}$ respectively, are axi-symmetric tensors, and, therefore, that the tensor form defined by each of them remains invariant under the full rotation group which includes proper and improper rotations (i.e. the orthogonal group O[3]) with respect to the axial direction[‡]. We, therefore, also assume that

Assumption 2:

$$H_{\nu j,\mu l}(\underline{y},\underline{\eta},\omega) \textit{ is an axi-symmetric tensor} \tag{17}$$

These two assumptions, which (as Afsar *et al* [2]) we again refer to as *statistical axi-symmetry*, leads to the following approximation:

$$H_{\nu j,\mu l}(\underline{y},\eta_1,\underline{\eta}_\perp,\omega) \approx H_{\nu j,\mu l}(\underline{y},\eta_1,|\underline{\eta}_\perp|,\omega) \textit{ is an axi-symmetric tensor} \tag{18}$$

It is now easy to show from (8) that that the tensor in (8) (i.e. $\mathcal{H}_{\nu j,\mu l}(\underline{y},\underline{\eta},\omega)$), which actually enters (4), is also statistically axi-symmetric, i.e. that

$$\mathcal{H}_{\nu j,\mu l}(\underline{y},\eta_1,\underline{\eta}_\perp,\omega) \approx \mathcal{H}_{\nu j,\mu l}(\underline{y},\eta_1,|\underline{\eta}_\perp|,\omega) \tag{19}$$

is an axi-symmetric tensor.

---

‡ Under a more general definition of axi-symmetry, the representation of the tensor of odd parity $R_{4j,kl}$ would be such that its tensor form is invariant to proper rotations only (see Afsar [17]).

3.2. Spectral tensor formalism

Observations reported in Harper-Bourne [62] and Pokora & McGuirk [63] indicate that the streamwise and transverse turbulence correlation lengths are short compared to the corresponding mean flow length scales (especially at the end of the potential core which is the region of most importance for the results in this paper). Appendix B shows that this disparity can be exploited to simplify the formula for the acoustic spectrum by using the WKBJ approximation to account the variations of the propagator $\Gamma^*_{\mu l}(\underline{x} \mid \underline{y} + \underline{\eta}; \omega)$ over the turbulence correlation volume. Equation (B5) can be inserted into equation (15) to show that the three components of the far-field acoustic spectrum $I_\omega(\underline{x} \mid \underline{y})$ are given by the purely algebraic results:

$$I^{[1]}_\omega(\underline{x} \mid \underline{y}) \approx G_{ij}(\underline{x} \mid \underline{y}; \omega) G^*_{kl}(\underline{x} \mid \underline{y}; \omega) \Phi^*_{ij,kl}\left(\underline{y}, \underline{k}, \omega\right) \tag{20a}$$

$$I^{[2]}_\omega(\underline{x} \mid \underline{y}) \approx 2\mathrm{Re}\left\{\Gamma_{4j}(\underline{x} \mid \underline{y}; \omega) G^*_{kl}(\underline{x} \mid \underline{y}; \omega) \Phi^*_{4j,kl}\left(\underline{y}, \underline{k}, \omega\right)\right\} \tag{20b}$$

$$I^{[3]}_\omega(\underline{x} \mid \underline{y}) \approx \Gamma_{4j}(\underline{x} \mid \underline{y}; \omega) \Gamma^*_{4l}(\underline{x} \mid \underline{y}; \omega) \Phi^*_{4j,4l}\left(\underline{y}, \underline{k}, \omega\right) \tag{20c}$$

where, $\underline{k} = \dfrac{\omega}{c_\infty} \underline{\nabla}_{\underline{y}} S(\underline{x} \mid \underline{y})$. Equation (20) depends on the turbulence correlations only through the complex conjugate of the fourth rank spectral tensor $\Phi_{\nu j,\mu l}(\underline{y}, k_1, \underline{k}_\perp, \omega)$, which is related to the Reynolds stress auto-covariance tensor (7) by (8), (9) and the Fourier transform

$$\Phi_{\nu j,\mu l}(\underline{y}, k_1, \underline{k}_\perp, \omega) = \int_{\underline{\eta}} \mathcal{H}_{\nu j,\mu l}(\underline{y}, \underline{\eta}, \omega) e^{-i\underline{k}.\underline{\eta}} \, d\underline{\eta}. \tag{21}$$

The wave vector $\underline{k}$ is defined by its Cartesian components $\underline{k} = (k_1, \underline{k}_\perp)$, where k_1 is the axial component and $\underline{k}_\perp$ is in the transverse direction. $\mathcal{H}_{\nu j,\mu l}(\underline{y}, \underline{\eta}, \omega)$ is related to the Reynolds stress auto-covariance through equations (8) -- (10), and $\underline{k}_\perp$ can be identified with $(\omega/c_\infty)\underline{\nabla}_\perp S(\underline{x} \mid \underline{y})$ using (B5). It is important to note that it would be impossible to define the Fourier transform (21) if the auto-covariance tensor (7) were replaced by the correlation tensor

$$\frac{1}{2T}\int_{-T}^{+T} \rho v'_\nu v'_j(\underline{y}, \tau)\rho v'_\mu v'_l(\underline{y} + \underline{\eta}, \tau + \tau_0)\, d\tau, \tag{22}$$

as is frequently done in analyses based on a Lilley-type equation since, as pointed out by Batchelor ([55], p.179), the latter quantity tends to a non-zero value as $|\underline{\eta}| \to \infty$.

It now follows from the symmetry properties of $H_{\nu j,\mu l}(\underline{y}, \underline{\eta}, \omega)$ that the spectral tensor components have different symmetries in each of the three terms in (20) which are summarized in table (1).

	Spectral tensor components	**Symmetries**	**Number of independent terms**
Momentum flux term $I_\omega^{[1]}(\underline{x} \mid \underline{y})$	$\Phi^*_{ij,kl}$	2 pair symmetries: $(i \leftrightarrow j)\ \ (k \leftrightarrow l)$	36
Enthalpy flux – momentum flux coupling term $I_\omega^{[2]}(\underline{x} \mid \underline{y})$	$\Phi^*_{4j,kl}$	1 pair symmetry: $(k \leftrightarrow l)$	18
Enthalpy flux term $I_\omega^{[3]}(\underline{x} \mid \underline{y})$	$\Phi^*_{4j,4l}$	No symmetries.	9

Table 1: Symmetries of the three terms in acoustic spectrum equation (20)

It is easy to show that the Fourier transform $\Phi^*_{\nu j,\mu l}(\underline{y}, k_1, \underline{k}_\perp, \omega)$ of $\mathcal{H}_{\nu j,\mu l}(\underline{y}, \eta_1, \underline{\eta}_\perp, \omega)$ will depend only on the magnitude squared $k_\perp^2$ of the transverse wave number $\underline{k}_\perp$ when $\mathcal{H}_{\nu j,\mu l}(\underline{y}, \eta_1, \underline{\eta}_\perp, \omega)$ satisfies (19); i.e., that

$$\Phi^*_{\nu j,\mu l}(\underline{y}, k_1, \underline{k}_\perp, \omega) \approx \Phi^*_{\nu j,\mu l}(\underline{y}, k_1, k_\perp^2, \omega), \tag{23}$$

where $k_\perp^2 = k_2^2 + k_3^2$. *It is also easy to show that the Fourier transform,* $\Phi^*_{\nu j,\mu l}(\underline{y}, k_1, k_\perp^2, \omega)$, *of* $\mathcal{H}_{\nu j,\mu l}(\underline{y}, \eta_1, |\underline{\eta}_\perp|, \omega)$ *is an axi-symmetric tensor with respect to the wave number vector* $\underline{k}$ *in the sense that the tensor form defined by each of the three tensors* $\Phi^*_{ij,kl}, \Phi^*_{4j,kl}, \Phi^*_{4j,4l}$ remains invariant under the full rotation group with respect to the k_1–direction, when $\mathcal{H}_{\nu j,\mu l}(\underline{y}, \eta_1, |\underline{\eta}_\perp|, \omega)$ is an axi-symmetric tensor. So it follows that $\Phi_{\nu j,\mu l}(\underline{y}, k_1, \underline{k}_\perp, \omega)$ must satisfy the statistical axi-symmetry property if the original generalized auto-covariance tensor $R_{\nu j,\mu l}(\underline{y}, \eta_1, \underline{\eta}_\perp, \tau_0)$ has this property—but now in terms of the wave number vector $\underline{k}$ instead of the separation vector $\underline{\eta}$.

In total $\Phi^*_{\nu j,\mu l}(\underline{y}, k_1, k_\perp^2, \omega)$ possesses 63 independent components. The three contributions to the acoustic spectrum are then given by:

$$I_\omega^{[1]}(\underline{x} \mid \underline{y}) \approx G_{ij}(\underline{x} \mid \underline{y}; \omega) G^*_{kl}(\underline{x} \mid \underline{y}; \omega) \Phi^*_{ij,kl}(\underline{y}, k_1, k_\perp^2, \omega) \tag{24a}$$

$$I_\omega^{[2]}(\underline{x} \mid \underline{y}) \approx 2\mathrm{Re}\left\{\Gamma_{4j}(\underline{x} \mid \underline{y}; \omega) G^*_{kl}(\underline{x} \mid \underline{y}; \omega) \Phi^*_{4j,kl}(\underline{y}, k_1, k_\perp^2, \omega)\right\} \tag{24b}$$

$$I_\omega^{[3]}(\underline{x} \mid \underline{y}) \approx \Gamma_{4j}(\underline{x} \mid \underline{y}; \omega) \Gamma^*_{4l}(\underline{x} \mid \underline{y}; \omega) \Phi^*_{4j,4l}(\underline{y}, k_1, k_\perp^2, \omega) \tag{24c}$$

4. CONTRIBUTIONS TO THE ACOUSTIC SPECTRUM

Appendix C shows the application of approximations 1 and 2 reduces the total number of independent components of $\Phi^*_{\nu j,\mu l}(\underline{y}, k_1, k_\perp^2, \omega)$ from 63 to only 11. Inserting equation (C4) into (24a) shows that the far field acoustic spectrum $I^{[1]}_\omega\ (\underline{x} \mid \underline{y})$ is given by:

$$
\begin{aligned}
I^{[1]}_\omega(\underline{x} \mid \underline{y}) \approx & \left[G_{ii}G^*_{kk} - 2\mathrm{Re}(G_{11}G^*_{kk}) + G_{11}G^*_{11}\right]\Phi^*_{22,22}(\underline{y}, \underline{k}, \omega) \\
& + \mathrm{Re}\left[G_{11}G^*_{kk} - G_{11}G^*_{11}\right]\left(\Phi^*_{11,22} + \Phi^*_{22,11}\right)(\underline{y}, \underline{k}, \omega) \\
& + G_{11}G^*_{11}\Phi^*_{11,11}(\underline{y}, \underline{k}, \omega) \\
& + 2\left[G_{ik}G^*_{ik} - G_{ii}G^*_{kk} + 2\mathrm{Re}(G_{11}G^*_{kk}) - 2G_{k1}G^*_{k1}\right]\Phi^*_{23,23}(\underline{y}, \underline{k}, \omega) \\
& + 4\left[G_{k1}G^*_{k1} - G_{11}G^*_{11}\right]\Phi^*_{12,12}(\underline{y}, \underline{k}, \omega)
\end{aligned}
\tag{25}
$$

The $\Phi^*_{23,23}$ spectral tensor component can be re-written using the spectral version of Millionshchikov's identity, which is satisfied by equation (C4) (see Afsar *et al* [2]) and the result can be rearranged to obtain the following remarkably simple formula for $I^{[1]}_\omega\ (\underline{x} \mid \underline{y})$.

$$
\begin{aligned}
I^{[1]}_\omega(\underline{x} \mid \underline{y}) \approx & \left[|G_{22}|^2 + |G_{33}|^2 + 2|G_{23}|^2\right]\Phi^*_{22,22} + \mathrm{Re}\left[G_{11}(G^*_{22} + G^*_{33})\right]\left(\Phi^*_{11,22} + \Phi^*_{22,11}\right) \\
& + |G_{11}|^2\Phi^*_{11,11} + 2\left[\mathrm{Re}\left(G_{22}G^*_{33}\right) - |G_{23}|^2\right]\Phi^*_{22,33} + 4\left[|G_{12}|^2 + |G_{13}|^2\right]\Phi^*_{12,12},
\end{aligned}
\tag{26}
$$

where the arguments of the symmetric propagator, G_{ij}, are $(\underline{x} \mid \underline{y}; \omega)$ and the components of spectral tensor are functions of $(\underline{y}, k_1, k_2^2 + k_3^2, \omega)$. Equation (26) applies to jets of any cross section and does not require that the mean flow (which enters through the propagators G_{ij}) be parallel or even weakly non-parallel. It is a generalization of equation (6.27) in [9] and

depends on the six independent components $\Phi^*_{22,22}$, $\Phi^*_{11,22}$, $\Phi^*_{22,11}$, $\Phi^*_{11,11}$, $\Phi^*_{22,33}$ and $\Phi^*_{12,12}$, of the spectral tensor $\Phi^*_{ij,kl}$ which are related to the components of the Reynolds stress auto-covariance tensor by equation by (8), (9) and (21). Further analysis of the properties of equation (26) can be found in Afsar [17].

Substituting (C7) into (24b) and (C8) into (24c) shows that the enthalpy terms $I^{[2]}_{\omega}\left(\underline{x} \mid \underline{y}\right)$ and $I^{[3]}_{\omega}\left(\underline{x} \mid \underline{y}\right)$ can be expressed as

$$I^{[2]}_{\omega}\left(\underline{x} \mid \underline{y}\right) \approx 2\mathrm{Re}\left\{\Gamma_{41}G^*_0\Phi^*_{41,22} + \Gamma_{41}G^*_{11}\Phi^*_{41,11} + 2\left[\Gamma_{42}G^*_{12} + \Gamma_{43}G^*_{13}\right]\Phi^*_{42,21}\right\}, \tag{27}$$

$$I^{[3]}_{\omega}\left(\underline{x} \mid \underline{y}\right) \approx \left[|\Gamma_{42}|^2 + |\Gamma_{43}|^2\right]\Phi^*_{42,42} + |\Gamma_{41}|^2\Phi^*_{41,41}. \tag{28}$$

In the remainder of the paper recent flow measurements taken in the Small Hot Jet Acoustic Rig (SHJAR), located in the AeroAcoustic Propulsion Laboratory (AAPL) at NASA Glenn Research Center (GRC) (Mielke *et al*, [40] and [41]) are used to interpret the observed behavior of the far field acoustic spectrum, $I_{\omega}(\underline{x})$, but with particular attention to how $I^{[2]}_{\omega}$ and $I^{[3]}_{\omega}$ change with temperature ratio and acoustic Mach number.

5. TURBULENCE MEASUREMENTS IN HEATED JETS

A molecular Rayleigh scattering technique developed at (GRC) was used to measure gas velocity, temperature, and density at a sampling rate of 10 kHz in the SHJAR Rig (which is a vitiated air heated jet rig that uses a hydrogen combustor and central air compressor facilities, and can operated over a range of Mach numbers up to Mach 2, and static temperature ratios up to 2.8). The testing was done with a 50.8-mm exit diameter nozzle

with a smooth round exit. The experiments covered a range of acoustic Mach numbers from 0.5 to 1.59 and a range of static temperature ratios ($TR = T_{\text{jet}}/T_{\infty}$) from 0.835 to 2.7. A high power continuous-wave laser beam was focused at a point in the flow field and Rayleigh scattered light was collected and fiber-optically transmitted to a Fabry-Perot interferometer for spectral analysis. Photomultipler tubes operated in the photon counting mode were used to sample the total signal level and the circular interference pattern to provide simultaneous static density, static temperature, and axial velocity measurements. Some of the data from these experiments was reported in Khavaran *et al* [56], but this is the first time that it was used to analyze the covariance functions that appear in the coupling term. Measurements were acquired at several axial locations of $y_1/D_{\text{jet}} \geq 2$ and radial locations of $0.0 \leq r/D_{\text{jet}} \leq 1.25$.

Measurements were carried out at the temperature ratios and Mach numbers originally analyzed by Tanna [10] and summarized in table 2.

SETPOINT	NOZZLE	M	TR
7	SMC000	0.900	0.835
23	SMC000	0.500	1.765
27	SMC000	0.900	1.765
32	SMC000	0.500	2.270
42	SMC000	0.500	2.700
46	SMC000	0.900	2.700
49	SMC000	1.480	2.700

Table 2: Flow conditions and associated set point numbers used by Tanna [10].

Time-resolved Rayleigh scattering measurements of axial velocity, static temperature, and static density and the discrete correlation theorem (Press *et al* [57]) were used to calculate the fourth-rank correlation functions: $R_{11,11}(\underline{y},\underline{0},\tau_0)$, $R_{41,11}(\underline{y},\underline{0},\tau_0)$ and $R_{41,41}(\underline{y},\underline{0},\tau_0)$ defined in equations (7) and (11). The intermediate step involves the calculation the power spectrum, which provides a measure of the energy of the fluctuations in each frequency bin, and plays an important role in filtering noise from the data. Further details can be found in Mielke *et al* [40] and [41].

5.1. Amplitudes of the enthalpy-associated correlation functions

The $2\mathrm{Re}\{\Gamma_{41}G_{11}^{*}\Phi_{41,11}^{*}\}$ and $|\Gamma_{41}|^2\Phi_{41,41}^{*}$ terms in the $I_{\omega}^{[2]}$, $I_{\omega}^{[3]}$ components of (15) can be used to get a tentative idea of how these purely fluid mechanical effects of $R_{11,11}(\underline{y},\underline{0},0)$, $R_{41,11}(\underline{y},\underline{0},0)$ and $R_{41,41}(\underline{y},\underline{0},0)$ can influence the acoustic spectrum. Equation (5.20) of reference [9] shows that

$$I_{\omega}^{[2]}\left(\underline{x}\mid\underline{y}\right)\approx\left(\frac{\widetilde{c^2}}{c_{\infty}^2}\right)\frac{4\cos^3\theta}{\left[1-M(\underline{y}_{\perp})\cos\theta\right]^3}\frac{|\widetilde{\mathcal{G}}|^2}{c_{\infty}}\Phi_{41,11}^{*}, \tag{29}$$

and

$$I_{\omega}^{[3]}\left(\underline{x}\mid\underline{y}\right)\approx\frac{4\cos^2\theta}{\left[1-M(\underline{y}_{\perp})\cos\theta\right]^2}\frac{|\widetilde{\mathcal{G}}|^2}{c_{\infty}^2}\Phi_{41,41}^{*}. \tag{30}$$

for a parallel mean flow, where $(\widetilde{\mathcal{G}})$ denotes the scaled adjoint Lilley Green's function (defined by their equations (4.20) and (5.22) of reference [9]).

The Doppler factors that appear in these formulas arise from the propagator and, therefore, can only depend on the mean flow velocity and not on the source convection velocity. They tend to have a much larger effect at transonic speeds than those that would arise from source convection effects because they are raised to a high power and can be much closer to zero at small observation angles. And more importantly they can change sign at supersonic speeds while the source convection Doppler factor cannot—since the analysis has been restricted to subsonic convection Mach numbers. These are some of the most important differences between the present more exact approach and the Lighthill approach. They tend to become very significant at high Mach number and small observation angles.

Since $|\widetilde{\mathcal{G}}|^2$ has the dimensions of L^{-3}, where L is an appropriate length scale, these results imply that an appropriate normalization for $R_{41,11}$ and $R_{41,41}$ is:

$$\frac{R_{41,11}}{c_\infty R_{11,11}} \text{ and } \frac{R_{41,41}}{c_\infty^2 R_{11,11}} . \tag{31}$$

Figure (1) shows that $R_{41,11}$ becomes the same order as $R_{41,41}$ at high Mach number. This can be seen this more clearly in figure (2), which shows the individual correlation functions at various Mach numbers, at a fixed temperature ratio of 2.7.

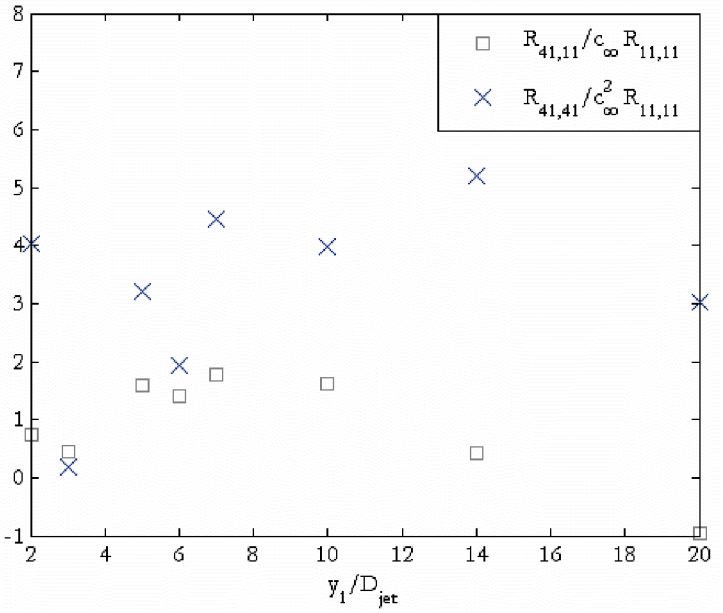

Figure 1a: SP46, $M = 0.90$.

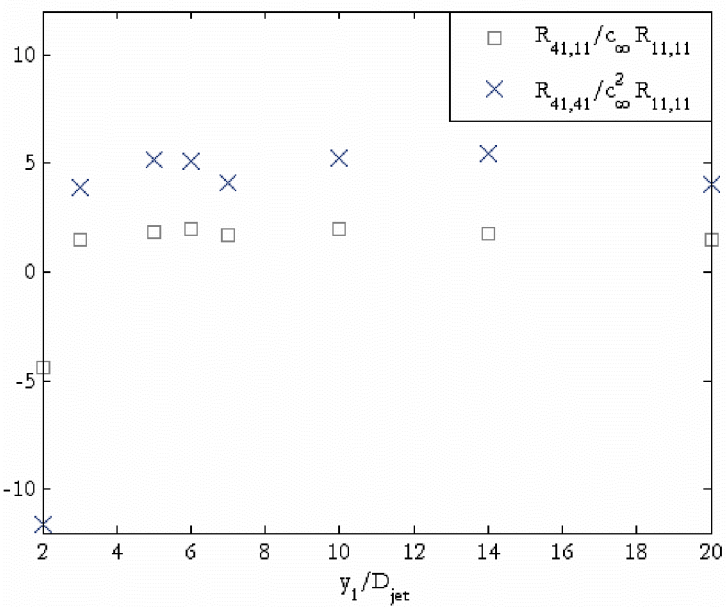

Figure 1b: SP49, $M = 1.48$.

FIGURE 1: Heated jet correlation functions at fixed temperature ratio of $TR = 2.70$ along the nozzle lip line.

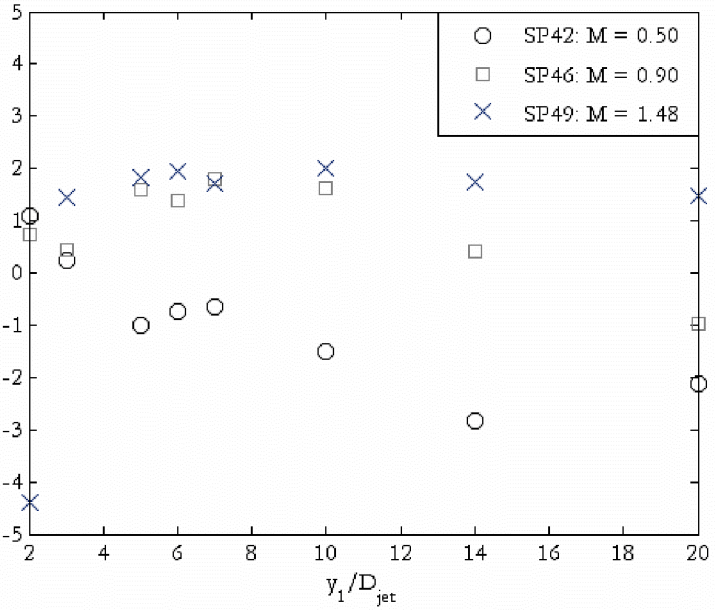

Figure 2a: $R_{41,11}/(c_\infty R_{11,11})$.

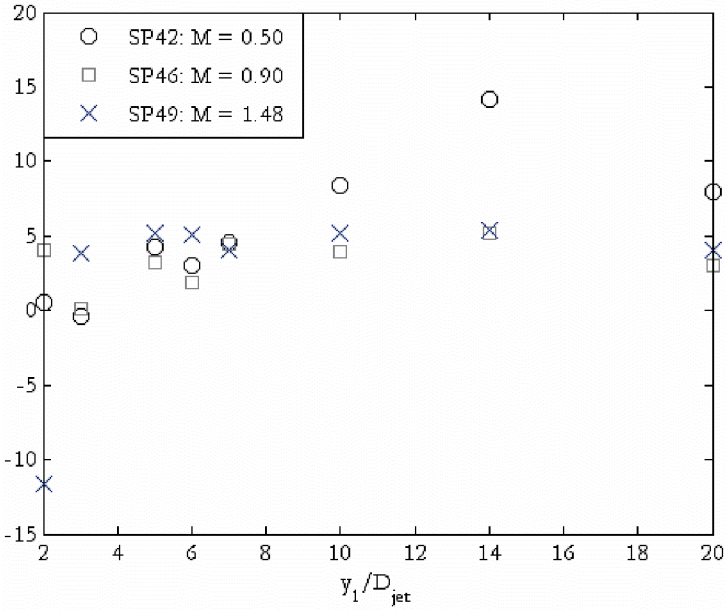

Figure 2b: $R_{41,41}/(c_\infty^2 R_{11,11})$.

FIGURE 2: Heated jet correlation functions at fixed temperature ratio of $TR = 2.70$ along the nozzle lip line.

The negative value of $R_{41,41}$ at $x/D_{\text{jet}} = 2$ (see figures 1b and 2b) could result from aliasing associated with the under sampling of the fluctuations, since the fluctuations close to nozzle exit would contain frequencies as high as 100 kHz, whereas the sample rate in the experiments is 10 kHz. The temperature measurements in the far downstream region ($x/D_{\text{jet}} > 10$) could be affected by Mie scattering of the signal from dust particles present in the flow (Mielke *et al* [40] and [41]). The most reliable data, therefore, lies in the region between x/D_{jet}=3 and x/D_{jet}=10. While the results show that the amplitude of $R_{41,11}$ can become negative within this region when the Mach number is small (figure 2a), they also show that it is always positive at the higher transonic and supersonic Mach numbers where $R_{41,11}$ is of the same order as $R_{41,41}$. At the low subsonic Mach numbers of figure (2b), $R_{41,41}$ (which exists in the enthalpy flux term equation 30) is seen to be large in magnitude between x/D_{jet}=3 and x/D_{jet}=10.

5.2. Mathematical structure of the coupling term

It follows that the coupling term is only likely to be important at the higher transonic and supersonic acoustic Mach numbers where $R_{41,11}$ is positive. In order to understand its effect on the acoustic spectrum it is necessary to consider its contribution to (29) which is proportional to spectral tensor component,

$$\Phi^{*}_{41,11}=\int_{\underline{\eta}} \left[\frac{(3-\gamma)}{2} H_{41,11} - (\gamma-1) H_{41,22}\right] (\underline{y}, \underline{\eta}, \omega)\, e^{-i\underline{k}.\underline{\eta}}\, d\underline{\eta} \qquad (32)$$

There is no available data on the space and time correlation and we were unable to obtain any estimates of these quantities from currently available LES results. But the second term

is almost certainly small compared to the first because the transverse scales and turbulence intensities are almost always much smaller than the corresponding streamwise quantities. In fact, it is not unreasonable to expect that the relative magnitudes of the Fourier transforms $H_{41,11}(\underline{y},\underline{\eta},\omega)$ and $H_{41,22}(\underline{y},\underline{\eta},\omega)$ are the same as the relative magnitudes of the corresponding $R_{11,11}(\underline{y},\underline{\eta},\tau_0)$ and $R_{11,22}(\underline{y},\underline{\eta},\tau_0)$ components of the Reynolds stress auto-covariance tensor. Since LES results reported in Karabasov *et al* [43] indicate that the ratio of the amplitude of the lateral co-variance $R_{11,22}(\underline{y},\underline{\eta},\tau_0)$, to $R_{11,11}(\underline{y},\underline{\eta},\tau_0)$, is less than 0.1 at the end of the potential core, it may be reasonable to suppose that the relative magnitudes of the Fourier transforms $H_{41,11}(\underline{y},\underline{\eta},\omega)$ and $H_{41,22}(\underline{y},\underline{\eta},\omega)$ behave similarly. This then implies that the square brackets in equation (32) is proportional to a positive constant times $H_{41,11}(\underline{y},\underline{\eta},\omega)$ and that $\Phi^*_{41,11}$ is, therefore, expected to be positive when the acoustic Mach number is transonic and supersonic. Since the propagator depends only on the mean flow and is unaffected by source convection, any Doppler factors that appear in this quantity must depend only on the mean flow. These (mean flow) Doppler factors would not appear in the Lighthill approach—which does not explicitly account for mean flow interaction effects. These factors can be much larger than the weaker source convection Doppler factors that occur in the Lighthill approach (as well as in the present approach) and can have a much stronger effect on the radiated sound when the convection velocity is subsonic but the acoustic Mach number is supersonic, as it is in the present result.

Equation (29) shows that for a parallel shear layer, $\Gamma_{41}G^*_{11}$ component of the propagator is proportional to 3 inverse (mean flow) Doppler factors, and can, therefore, change sign when the acoustic Mach number is supersonic and the observation point is close to the downstream jet axis. But it can only become negative when the Mach number is

supersonic and the observation angle is within the 'zone of silence' of the parallel shear layer Green's function.

The $\Gamma_{41}G_{11}^{*}$ component of the propagator is always positive at high subsonic Mach numbers and, therefore, makes a positive (enhancement) contribution to the acoustic spectrum. Although the contribution made by the enthalpy flux term $I_{\omega}^{[3]}$ is always positive definite (see equation 28), for the parallel shear layer Green's function, it will not be as directive as the coupling term (especially for transonic flows where the inverse Doppler factors are much more intense at small angles). Equation (30) shows, $I_{\omega}^{[3]}$ has a pre-factor with two inverse (mean flow) Doppler factors, and a leading multiplier of $\cos^2\theta$, whereas the propagator component multiplying $\Phi_{41,11}^{*}$ (equation 29) is proportional to three inverse (mean flow) Doppler factors and has a $\cos^3\theta$ multiplier.

When the Mach number is supersonic, the propagator $\Gamma_{41}G_{11}^{*}$ changes sign at small observation angles to the jet axis, so that the contribution made by the component (29) to the coupling term $I_{\omega}^{[2]}$ is negative. Analysis of the other terms in equation (27) shows that propagator that multiplies $\Phi_{42,21}^{*}$ possesses 5 inverse Doppler factors for the parallel shear layer Green's function. If the sign changes in the spectral tensor component $\Phi_{42,21}^{*}$ are the same as $\Phi_{41,11}^{*}$ with Mach number (at constant temperature ratio), this term could introduce even more cancellation, since it is almost as directive as the term that dominates the momentum flux term at small observation angles (see reference [9]).

This is the first time a *cancellation effect* brought about through the coupling between enthalpy flux and momentum flux has been highlighted. This cancellation effect has the potential of directly reducing the peak jet noise since the sign change in the propagator occurs at angles within the 'zone of silence' of $|\widetilde{\mathcal{G}}|^2$.

6. CONCLUSIONS

A self consistent approach to modeling jet noise in heated flows was developed in this paper. The starting point was the generalized form of the acoustic analogy derived by in [1], which allowed the acoustic spectrum to be expressed as the sum of three terms: the momentum flux auto-covariance term, the enthalpy flux – momentum flux covariance (or the coupling term) and the enthalpy flux auto-covariance. The statistical axi-symmetry model developed by Afsar *et al* [2] for the momentum flux auto-covariance was extended to the coupling term and enthalpy flux auto-covariance. This reduced the total number of independent terms in the acoustic spectrum formula from 63 down to 11. The main focus of the paper was on the coupling term, which was not considered in previous jet noise models. Recent Rayleigh scattering measurements taken at NASA Glenn were used to show the coupling term becomes increasingly important as the Mach number increases. Examination of its mathematical structure showed that it can provide either an enhancement, or a cancellation, depending on the acoustic Mach number and the position of the observation point relative to the jet axis.

The acoustic spectrum formula, given by equations (26) – (28), can be used for jet noise prediction, when the turbulence correlations are determined from either a computational solution (such as a large eddy simulation) or experimental data.

Acknowledgments

M. Z. A anknowledges the financial support from the NASA Post-doctoral program. The authors would also like to thank collegues at NASA, Drs. James Bridges, Abbas Khavaran and Stewart Leib for helpful discussions on the heated jet problem.

APPENDICES

A: SUMMARY OF AFSAR *ET AL* [2]

Afsar *et al* [2] showed that the statistical axi-symmetry assumption implies that the three components of the Reynolds stress auto-covariance tensor are related to one another by the Millionshchikov identity:

$$R_{22,22}(\underline{y},\eta_1,|\underline{\eta}_\perp|,\tau_0) = R_{22,33}(\underline{y},\eta_1,|\underline{\eta}_\perp|,\tau_0) + 2R_{23,23}(\underline{y},\eta_1,|\underline{\eta}_\perp|,\tau_0) \qquad \text{(A1)}$$

Figure A1 is a plot of $R_{22,22}(\underline{y},\eta_1,\tau_0)\,/R_{22,22}(\underline{y},\underline{0},0)$ as a function of τ_0 for various axial separations. The lines (solid, dashed, dot-dashed) are computed from the PIV data of Pokora & McGuirk [53] and the filled symbols are corresponding quantities calculated from the Millionshchikov identity (A1) with $R_{22,33}(\underline{y},\eta_1,\tau_0)$ and $R_{23,23}(\underline{y},\eta_1,\tau_0)$ computed from the same PIV data.

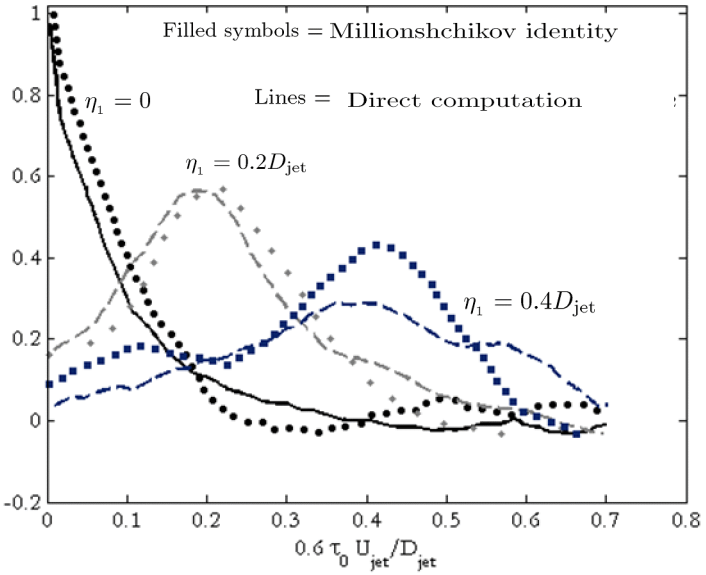

Figure A1a: $y_1/D_{\text{jet}} = 4$, $r/D_{\text{jet}} = 0.5$

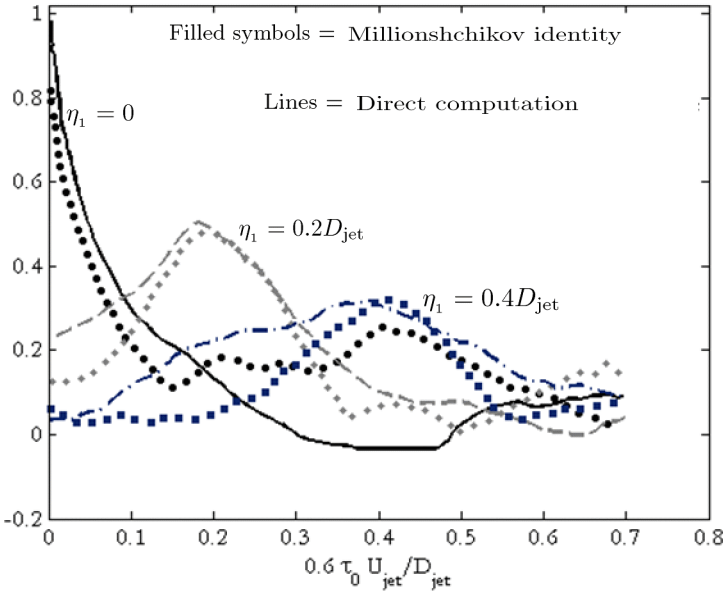

Figure A1b: $y_1/D_{\text{jet}} = 6.5$, $r/D_{\text{jet}} = 0.5$

Figure A.1: Millionshchikov identity (equation A1) normalized by $R_{22,22}(\underline{y}, \underline{0}, 0)$ is shown by the filled symbols, and compared to the direct evaluation of $R_{22,22}(\underline{y}, \underline{\eta}, \tau_0)/R_{22,22}(\underline{y}, \underline{0}, 0)$ shown in the solid lines.

B: TRANSVERSE VARIATIONS OF RETARDED TIME IN THE PROPAGATOR, $\Gamma^*_{\mu l}(\underline{x} \mid \underline{y} + \underline{\eta}; \omega)$

Significant simplification can be obtained if the propagator is taken outside of the integral in equation (15). But this amounts to neglecting variations of the Green's function over the turbulence correlation region, or neglecting the so-called 'retarded time' effects. It is now known that these effects can give rise to subtle source cancellations and neglecting them completely can lead to errors in the noise predictions.

Measurements taken by Pokora & McGuirk [53] seem to suggest that the transverse correlation lengths will be small relative to the transverse mean flow length scales, especially at the end of potential core, which is the region of primary interest here. We, therefore, assume that the turbulence correlation lengths are short compared to the corresponding transverse and streamwise length scales of the mean flow, say D_{jet} and L respectively, and exploit this length scale disparity to simplify the formula for the acoustic spectrum. Although the streamwise distance over which these fluctuations are correlated tends to be longer than the corresponding transverse distances, the mean flow varies much more slowly in the streamwise direction than in the transverse direction in high Reynolds number flows of interest in jet noise applications.

Since the linear equation governing the far field adjoint Green's function depends only on the mean flow and reduces to the wave equation outside the source region, its solution can only depend on the mean flow length scales (which enter through the coefficients of the equation) and the acoustic length scale or wave length c_∞/ω (since only the acoustic waves reach the far field). When these lengths are all large compared to the turbulence correlation lengths, the adjoint Green's function (and therefore the propagator) will be relatively constant over the correlation volume, and may, therefore, be moved outside

the integral over the separation vector in (15). But these variations cannot be neglected when any of these length scales is the order of, or smaller, than the correlation length, which in view of the above assumption, can only occur when acoustic wavelength c_∞/ω is small relative to D_{jet}. The Helmholtz number, $H = \omega D_{\text{jet}}/c_\infty$ (which is the ratio of the transverse mean flow length scale to the acoustic wave length), will then be large and the propagator $\Gamma^*_{\mu l}(\underline{x} \mid \underline{z}; \omega)$ can then therefore be represented by its high frequency, or WKBJ approximation (Khavaran [58])

$$\Gamma^*_{\mu l}(\underline{x} \mid \underline{z}; \omega) \approx A_{\mu l}(\underline{x} \mid \underline{\tilde{z}}; H) \exp\left[iHS(\underline{x} \mid \underline{\tilde{z}})\right]. \tag{B1}$$

whenever it does not remain constant over the correlation volume. Here $\underline{\tilde{z}} = (z_1/L, \underline{z}_\perp/D_{\text{jet}})$ is a scaled dummy variable that varies on the mean flow length scales and $A_{\mu l}(\underline{x} \mid \underline{z}; \omega)$ expands as a power series in inverse powers of H; i.e.

$$A_{\mu l}(\underline{x} \mid \underline{\tilde{z}}; H) = HA^{(0)}_{\mu l}(\underline{x} \mid \underline{\tilde{z}}) + A^{(1)}_{\mu l}(\underline{x} \mid \underline{\tilde{z}}) + \frac{1}{H}A^{(2)}_{\mu l}(\underline{x} \mid \underline{\tilde{z}}) + \left(\frac{1}{H}\right)^2 A^{(3)}_{\mu l}(\underline{x} \mid \underline{\tilde{z}})... \tag{B2}$$

The phase factor $S(\underline{x} \mid \underline{\tilde{z}})$ in equation (B1), which satisfies the usual Eikonal equation (Goldstein [59]), and the amplitudes $A_{\mu l}$ can be expanded in Taylor series to obtain

$$S(\underline{x} \mid \underline{\tilde{y}} + \underline{\tilde{\eta}}) = S(\underline{x} \mid \underline{\tilde{y}}) + \tilde{\eta}_i \frac{\partial S(\underline{x} \mid \underline{\tilde{y}})}{\partial \tilde{y}_i} + \tilde{\eta}_i\tilde{\eta}_j \frac{\partial^2 S(\underline{x} \mid \underline{\tilde{y}})}{\partial \tilde{y}_i \partial \tilde{y}_j} + ... \tag{B3a}$$

$$A_{\mu l}(\underline{x} \mid \underline{\tilde{y}} + \underline{\tilde{\eta}}; H) = A_{\mu l}(\underline{x} \mid \underline{\tilde{y}}; H) + \tilde{\eta}_i \frac{\partial A_{\mu l}(\underline{x} \mid \underline{\tilde{y}}; H)}{\partial \tilde{y}_i} + \tilde{\eta}_i\tilde{\eta}_j \frac{\partial^2 A_{\mu l}(\underline{x} \mid \underline{\tilde{y}}; H)}{\partial \tilde{y}_i \partial \tilde{y}_j} + ... \tag{B3b}$$

But since $\underline{y}$ varies on the slow scales D_{jet} & L of the mean flow, $A_{\mu l}(\underline{x} \mid \tilde{\underline{y}} + \tilde{\underline{\eta}}; H)$ and $S(\underline{x} \mid \tilde{\underline{y}} + \tilde{\underline{\eta}})$ can be well represented over the entire turbulence correlation volume $V_\infty(\underline{\eta})$ by the first term and the first two terms of their respective series. It, therefore, follows that:

$$S(\underline{x} \mid \tilde{\underline{y}} + \tilde{\underline{\eta}}) = S(\underline{x} \mid \tilde{\underline{y}}) + \tilde{\eta}_i \frac{\partial S(\underline{x} \mid \tilde{\underline{y}})}{\partial \tilde{y}_i} \tag{B4a}$$

and

$$A_{\mu l}(\underline{x} \mid \tilde{\underline{y}} + \tilde{\underline{\eta}}; H) = A_{\mu l}(\underline{x} \mid \tilde{\underline{y}}; H) \tag{B4b}$$

for variations on the scale of the correlation volume. Substituting these expressions into equation (B1) and using equation (B2) shows that

$$\Gamma^*_{\mu l}(\underline{x} \mid \underline{y} + \underline{\eta}; \omega) \approx \Gamma^*_{\mu l}(\underline{x} \mid \tilde{\underline{y}}; \omega) \exp\left[iH\tilde{\underline{\eta}}.\underline{\nabla}_{\tilde{\underline{y}}} S(\underline{x} \mid \tilde{\underline{y}})\right]. \tag{B5}$$

when $H \gg 1$ and, therefore, that

$$\int_{V_\infty(\underline{\eta})} \Gamma^*_{\mu l}(\underline{x} \mid \underline{y} + \underline{\eta}; \omega) \mathcal{H}_{\nu j,\mu l}(\underline{y}, \underline{\eta}, \omega)\, d\underline{\eta} \approx \Gamma^*_{\mu l}(\underline{x} \mid \underline{y}; \omega) \Phi^*_{\nu j,\mu l}(\underline{y}, \underline{k}, \omega), \tag{B6}$$

where $\Phi^*_{\nu j,\mu l}(\underline{y}, \underline{k}, \omega)$ is defined by equation (21), and

$$\Gamma^*_{\mu l}(\underline{x} \mid \underline{y}; \omega) = A_{\mu l}(\underline{x} \mid \tilde{\underline{y}}; H) \exp\left[iHS(\underline{x} \mid \tilde{\underline{y}})\right] \tag{B7}$$

is the high frequency approximation to $\Gamma^*_{\mu l}(\underline{x} \mid \underline{y}; \omega)$. But the approximation (B6) will also be valid for $O(1)$ frequencies when $\Gamma^*_{\mu l}(\underline{x} \mid \underline{y}; \omega)$ is interpreted to be the $O(1)$ frequency result in (B5), because $H\underline{\tilde{\eta}}$ will be small for variations on the scale of the correlation volume, and $\Gamma^*_{\mu l}(\underline{x} \mid \underline{y}; \omega)$ will only involve length scales that are large compared to the correlation volume and can therefore be factored out of the integral over that volume.

C. KINEMATIC THEORY: STATISTICAL AXI-SYMMETRY IN $\Phi^*_{\nu j,\mu l}(\underline{y}, k_1, k_\perp^2, \omega)$

C.1. Momentum flux term, $I^{[1]}_{\omega}(\underline{x} \mid \underline{y})$

The basic invariants in the axi-symmetric model of $\Phi^*_{ij,kl}(\underline{y}, k_1, k_\perp^2, \omega)$ consists of all terms of the form $(\delta_{ij}\delta_{kl}, \delta_{ij}\delta_{k1}\delta_{l1}, \delta_{i1}\delta_{j1}\delta_{k1}\delta_{l1})$ with the tensor suffixes taking on all possible values of (i, j, k, l), since $k_\perp^2$ enters this tensor only as scalar. So following the same procedure used in Afsar *et al* [2] for the real space tensor $R_{ij,kl}(\underline{y}, \eta_1, \underline{\eta}_\perp, \tau_0)$, the spectral tensor under statistical axi-symmetry $\Phi^*_{ij,kl}(\underline{y}, k_1, k_\perp^2, \omega)$ is

$$\begin{aligned}
\Phi^*_{ij,kl}(\underline{y}, k_1, k_\perp^2, \omega) = {} & \delta_{ij}\delta_{kl}A_1(\underline{y}, k^2, k_1, \omega) + \delta_{ik}\delta_{jl}A_2(\underline{y}, k^2, k_1, \omega) + \delta_{il}\delta_{jk}A_3(\underline{y}, k^2, k_1, \omega) \\
& + \delta_{i1}\delta_{j1}\delta_{kl}A_4(\underline{y}, k^2, k_1, \omega) + \delta_{k1}\delta_{l1}\delta_{ij}A_5(\underline{y}, k^2, k_1, \omega) \\
& + \delta_{i1}\delta_{k1}\delta_{jl}A_6(\underline{y}, k^2, k_1, \omega) + \delta_{j1}\delta_{l1}\delta_{ik}A_7(\underline{y}, k^2, k_1, \omega) \\
& + \delta_{i1}\delta_{l1}\delta_{jk}A_8(\underline{y}, k^2, k_1, \omega) + \delta_{j1}\delta_{k1}\delta_{il}A_9(\underline{y}, k^2, k_1, \omega) \\
& + \delta_{i1}\delta_{j1}\delta_{k1}\delta_{l1}A_{10}(\underline{y}, k^2, k_1, \omega), \qquad \text{(C1)}
\end{aligned}$$

where each scalar field depends upon the invariant $k^2 = k_i k_i = k_1^2 + k_\perp^2$ and k_1. Then since $\Phi^*_{ij,kl}$ is symmetric in the pairs, i.e. $\Phi^*_{ij,kl} = \Phi^*_{ji,kl}$ and $\Phi^*_{ij,kl} = \Phi^*_{ij,lk}$, this equation can be written as,

$$\begin{aligned}\Phi^*_{ij,kl}(\underline{y}, k_1, k_\perp^2, \omega) = {} & \delta_{ij}\delta_{kl}A_1(\underline{y}, k^2, k_1, \omega) + [\delta_{ik}\delta_{jl} + \delta_{il}\delta_{jk}]\, A_2(\underline{y}, k^2, k_1, \omega) \\ & + \ \delta_{i1}\delta_{j1}\delta_{kl}A_4(\underline{y}, k^2, k_1, \omega) + \delta_{k1}\delta_{l1}\delta_{ij}A_5(\underline{y}, k^2, k_1, \omega) \\ & + \ [\delta_{i1}\delta_{k1}\delta_{jl} + \delta_{j1}\delta_{l1}\delta_{ik} + \delta_{i1}\delta_{l1}\delta_{jk} + \delta_{j1}\delta_{k1}\delta_{il}]\, A_6(\underline{y}, k^2, k_1, \omega) \\ & + \ \delta_{i1}\delta_{j1}\delta_{k1}\delta_{l1}A_{10}(\underline{y}, k^2, k_1, \omega). \end{aligned} \tag{C2}$$

Substituting $(i, j, k, l) = (1, 2, 3)$ into equation (C2) shows that A_1, A_2, A_4, A_5, A_6 & A_{10} are related to the spectral tensor components by

$$A_1(\underline{y}, k^2, k_1, \omega) = \Phi^*_{22,22}(\underline{y}, k_1, k_\perp^2, \omega) - 2\Phi^*_{23,23}(\underline{y}, k_1, k_\perp^2, \omega) \tag{C3a}$$

$$A_2(\underline{y}, k^2, k_1, \omega) = \Phi^*_{23,23}(\underline{y}, k_1, k_\perp^2, \omega) \tag{C3b}$$

$$A_4(\underline{y}, k^2, k_1, \omega) = \Phi^*_{11,22}(\underline{y}, k_1, k_\perp^2, \omega) - \Phi^*_{22,22}(\underline{y}, k_1, k_\perp^2, \omega) + 2\Phi^*_{23,23}(\underline{y}, k_1, k_\perp^2, \omega) \tag{C3c}$$

$$A_5(\underline{y}, k^2, k_1, \omega) = \Phi^*_{22,11}(\underline{y}, k_1, k_\perp^2, \omega) - \Phi^*_{22,22}(\underline{y}, k_1, k_\perp^2, \omega) + 2\Phi^*_{23,23}(\underline{y}, k_1, k_\perp^2, \omega) \tag{C3d}$$

$$A_6(\underline{y}, k^2, k_1, \omega) = \Phi^*_{12,12}(\underline{y}, k_1, k_\perp^2, \omega) - \Phi^*_{23,23}(\underline{y}, k_1, k_\perp^2, \omega) \tag{C3e}$$

$$\begin{aligned} A_{10}(\underline{y}, k^2, k_1, \omega) = {} & \Phi^*_{11,11}(\underline{y}, k_1, k_\perp^2, \omega) + \Phi^*_{22,22}(\underline{y}, k_1, k_\perp^2, \omega) - \Phi^*_{11,22}(\underline{y}, k_1, k_\perp^2, \omega) \\ & - \Phi^*_{22,11}(\underline{y}, k_1, k_\perp^2, \omega) - 4\Phi^*_{12,12}(\underline{y}, k_1, k_\perp^2, \omega). \end{aligned} \tag{C3f}$$

$\Phi^*_{ij,kl}(\underline{y}, k_1, k_\perp^2, \omega)$, therefore, depends explicitly on six components: $\Phi^*_{11,11}$, $\Phi^*_{22,22}$, $\Phi^*_{12,12}$, $\Phi^*_{23,23}$, $\Phi^*_{11,22}$ & $\Phi^*_{22,11}$ and equation (C2) can be re-written as

$$\Phi^*_{ij,kl}(\underline{y},k_1,k_\perp^2,\omega) = \left[\delta_{ij}\delta_{kl} - \delta_{i1}\delta_{j1}\delta_{kl} - \delta_{k1}\delta_{l1}\delta_{ij} + \delta_{i1}\delta_{j1}\delta_{k1}\delta_{l1}\right]\Phi^*_{22,22}(\underline{y},k_1,k_\perp^2,\omega)$$
$$+ \big[\delta_{ik}\delta_{jl} + \delta_{il}\delta_{jk} - 2\delta_{ij}\delta_{kl} + 2\delta_{i1}\delta_{j1}\delta_{kl} + 2\delta_{k1}\delta_{l1}\delta_{ij}$$
$$- \delta_{i1}\delta_{l1}\delta_{jk} - \delta_{j1}\delta_{l1}\delta_{ik} - \delta_{j1}\delta_{k1}\delta_{il} - \delta_{i1}\delta_{k1}\delta_{jl}\big]\Phi^*_{23,23}(\underline{y},k_1,k_\perp^2,\omega)$$
$$+ \big[\delta_{i1}\delta_{l1}\delta_{jk} + \delta_{j1}\delta_{l1}\delta_{ik} + \delta_{j1}\delta_{k1}\delta_{il}$$
$$+ \delta_{i1}\delta_{k1}\delta_{jl} - 4\delta_{i1}\delta_{j1}\delta_{k1}\delta_{l1}\big]\Phi^*_{12,12}(\underline{y},k_1,k_\perp^2,\omega)$$
$$+ \left[\delta_{i1}\delta_{j1}\delta_{kl} - \delta_{i1}\delta_{j1}\delta_{k1}\delta_{l1}\right]\Phi^*_{11,22}(\underline{y},k_1,k_\perp^2,\omega)$$
$$+ \left[\delta_{k1}\delta_{l1}\delta_{ij} - \delta_{i1}\delta_{j1}\delta_{k1}\delta_{l1}\right]\Phi^*_{22,11}(\underline{y},k_1,k_\perp^2,\omega)$$
$$+ \delta_{i1}\delta_{j1}\delta_{k1}\delta_{l1}\Phi^*_{11,11}(\underline{y},k_1,k_\perp^2,\omega) \qquad \text{(C4)}$$

which implies that $\Phi^*_{22,22} = \Phi^*_{33,33}$, $\Phi^*_{11,22} = \Phi^*_{11,33}$ and $\Phi^*_{12,12} = \Phi^*_{13,13}$.

C.2. Enthalpy flux – momentum flux coupling term, $I^{[2]}_{\omega}(\underline{x} \mid \underline{y})$

Applying approximation 1 to the general 3rd rank axi-symmetric tensor given by equation 3.3.10 of Batchelor ([55], pp. 43), using a proof similar to the one given in Afsar *et al* [2] for the momentum flux term and applying the single pair symmetry shown in table (1) implies that

$$\Phi^*_{4j,kl}(\underline{y},k_1,k_\perp^2,\omega) =$$
$$= \delta_{j1}\delta_{kl}A_1(\underline{y},k^2,k_1,\omega) + (\delta_{k1}\delta_{jl} + \delta_{l1}\delta_{jk})\,A_2(\underline{y},k^2,k_1,\omega) + \delta_{j1}\delta_{k1}\delta_{l1}A_3(\underline{y},k^2,k_1,\omega) \qquad \text{(C5)}$$

Then since

$$A_1(\underline{y},k^2,k_1,\omega) = \Phi^*_{41,22}(\underline{y},k_1,k_\perp^2,\omega) \qquad \text{(C6a)}$$

$$A_2(\underline{y}, k^2, k_1, \omega) = \Phi^*_{42,21}(\underline{y}, k_1, k_\perp^2, \omega) \tag{C6b}$$

$$A_3(\underline{y}, k^2, k_1, \omega) = \Phi^*_{41,11}(\underline{y}, k_1, k_\perp^2, \omega) - \Phi^*_{41,22}(\underline{y}, k_1, k_\perp^2, \omega) - 2\Phi^*_{42,21}(\underline{y}, k_1, k_\perp^2, \omega) \tag{C6c}$$

the scalar fields in (C5) can be replaced by the components of $\Phi^*_{4j,kl}(\underline{y}, k_1, k_\perp^2, \omega)$ to obtain

$$\begin{aligned}\Phi^*_{4j,kl}(\underline{y}, k_1, k_\perp^2, \omega) = {} & (\delta_{j1}\delta_{kl} - \delta_{j1}\delta_{k1}\delta_{l1})\,\Phi^*_{41,22}(\underline{y}, k_1, k_\perp^2, \omega) \\ & + (\delta_{k1}\delta_{jl} + \delta_{l1}\delta_{jk} - 2\delta_{j1}\delta_{k1}\delta_{l1})\,\Phi^*_{42,21}(\underline{y}, k_1, k_\perp^2, \omega) \\ & + \delta_{j1}\delta_{k1}\delta_{l1}\Phi^*_{41,11}(\underline{y}, k_1, k_\perp^2, \omega)\end{aligned} \tag{C7}$$

which shows that $\Phi^*_{4j,kl}(\underline{y}, k_1, k_\perp^2, \omega)$ depends upon the 3 components: $\Phi^*_{41,11}$, $\Phi^*_{41,22}$ & $\Phi^*_{42,21}$ of $\Phi^*_{\nu j,\mu l}(\underline{y}, k_1, k_\perp^2, \omega)$. This result also implies that $\Phi^*_{41,22} = \Phi^*_{41,33}$ and $\Phi^*_{42,21} = \Phi^*_{43,31} = \Phi^*_{42,12} = \Phi^*_{43,13}$.

C.3. Enthalpy flux term, $I^{[3]}_\omega\ (\underline{x} \mid \underline{y})$

Although $\Phi^*_{4j,4l}(\underline{y}, k_1, k_\perp^2, \omega)$ does not, in general, possess any symmetries in its suffixes, approximation 2, introduces a pair symmetry in the suffixes (j, l). Applying approximation 1 to the 2nd rank axi-asymmetric tensor given by equation (3.3.9) of Batchelor ([55], pp. 43, shows that $\Phi^*_{4j,4l}(\underline{y}, k_1, k_\perp^2, \omega) = \delta_{j1}\delta_{l1}A_1(\underline{y}, k^2, k_1, \omega) + \delta_{jl}A_2(\underline{y}, k^2, k_1, \omega)$, which can then be re-written as:

$$\Phi^*_{4j,4l}(\underline{y}, k_1, k_\perp^2, \omega) = (\delta_{jl} - \delta_{j1}\delta_{l1})\,\Phi^*_{42,42}(\underline{y}, k_1, k_\perp^2, \omega) + \delta_{j1}\delta_{l1}\Phi^*_{41,41}(\underline{y}, k_1, k_\perp^2, \omega) \tag{C8}$$

where $\Phi^*_{42,42} = \Phi^*_{43,43}$ since

$$A_1(\underline{y}, k^2, k_1, \omega) = \Phi^*_{41,41}(\underline{y}, k_1, k_\perp^2, \omega) - \Phi^*_{42,42}(\underline{y}, k_1, k_\perp^2, \omega) \tag{C9a}$$

$$A_2(\underline{y}, k^2, k_1, \omega) = \Phi^*_{42,42}(\underline{y}, k_1, k_\perp^2, \omega) \tag{C9b}$$

REFERENCES

[1]. Goldstein, M. E. 2003. A generalized acoustic analogy. *J. Fluid Mech.* **488**, 315-333.

[2]. Afsar, M. Z., McGuirk, J. J. & Pokora, C. D. 2010. Statistical axi-symmetric model of the two-point time delayed auto-covariance of the Reynolds stress tensor. 19th Polish Fluid Mechanics Conference, Poznan, Poland.

[3]. Viswanathan, K. 2004. Aeroacoustics of hot jets. *J. Fluid Mech.* **516**, 39 – 82.

[4]. Tam, C. K. W. & Pastouchenko, N. N. 2005. Fine-Scale Turbulence from Hot Jets. *AIAA Journal* **43**, No. 8, 1675 – 1683.

[5]. Bodony, D. J. & Lele, S. K. 2005. On using large-eddy simulation for the prediction of noise from cold and heated jets. *Phys. Fluids* **17**, 085103.

[6]. Lush, P. A. & Fischer, M. J. 1973. Noise from hot jets. AGARD CP-131. Noise mechanisms, chapter 12.

[7]. Morfey, C. L., Szewczyk, V. M. & Tester, B. J. 1978. New scaling laws for hot and cold jet mixing noise based on a geometric acoustics model. *J. Sound Vib.* **61**, 255 – 292.

[8]. Lilley, G. M. 1996. The sound radiated from isotropic turbulence with application to the theory of jet noise. *J. Sound Vib.* **190**, No. 3, 463 – 476.

[9]. Goldstein, M. E. & Leib, S. J. 2008. The aeroacoustics of slowly divereging supersonic jet flows. *J. Fluid Mech.* **600**, 291 – 337.

[10]. Tanna, H. K. 1977. An experimental study of jet noise. Part I: Turbulent mixing noise. *J. Sound Vib.* **50**, No. 3, 405 – 428.

[11]. Harper-Bourne, M. 2007. Some observations on the noise of heated jets. AIAA-2007-3632, 13th AIAA/CEAS Aeroacoustics Conference, Rome, Italy.

[12]. Tester, B. J. & Morfey, C. L. 2009. Jet mixing noise: a review of single stream temperature effects. AIAA 2009-3376.

[13]. Viswanathan, K. 2009. Mechanisms of jet noise generation: classical theories and recent developments. *Int. J. Aeroacoustics* **8**, No. 4, 355 – 408.

[14]. Andersson, N. 2003. A study of Mach 0.75 jets and their radiated sound using Large-eddy simulation. PhD thesis, Chalmers University of Technology, Sweden.

[15]. Moore, P. D., Slot, H. J. & Boersma, B. J. 2007. Direct numerical simulation of low Reynolds number hot and cold jets. AIAA 2007-3631.

[16]. Bodony, D. J. & Lele, S. K. 2008. Low frequency sound sources in high-speed turbulent jets. *J. Fluid Mech.* **617**, 231 – 253.

[17]. Afsar, M. Z. 2010. A complete theoretical foundation for the "two-source" structure of jet noise. International Congress of Mathematicians, Hyderabad, India.

[18]. Lighthill, M. J. 1952. On sound generated aerodynamically: I. General theory. *Proc. Roy. Soc.* A, **222**, 564-587.

[19]. Lassiter, L. W. & Hubbard, H. H. 1952. Experimental studies of noise from subsonic jets in still air. Technical report, NACA, TN-2757 NACA.

[20]. Rollin, V. G. 1958. The effect of jet temperature on jet noise generation. NACA TN-4217.

[21]. Hoch, R. G., Duponchel, J. P., Cocking, B. J. & Bryce, W. D. 1973. Studies of the influence of density on jet noise. *J. Sound Vib.* **28**, 649 – 668.

[22]. Witze, P. O. 1974. Centerline velocity decay of compressible free jets. *AIAA Journal* **12**, No. 4, 417 – 418.

[23]. Cocking, B. J. 1974. The effect of temperature on subsonic jet noise. National gas turbine establishment, NGTE Rep. R. 331. Cited in Harper-Bourne, 2007.

[24]. Antonia, R. A. & Van Atta, C. W. 1975. *J. Fluid Mech.* **67**, 273.

[25]. Tanna, H. K., Dean, P. D. & Fischer, M. J. 1975. The influence of temperature on shock-free supersonic jet noise. *J. Sound Vib.* **39**, 429 – 460.

[26]. Tester, B. J. & Morfey, C. L. 1976. Developments in jet noise modeling – theoretical predictions and comparisons with measured data. *J. Sound Vib.* **46**, 79 – 103.

[27]. Lau, J. C. 1981. Effects of exit Mach number and temperature on mean-flow and turbulence characteristics in round jets. *J. Fluid Mech.* **105**, 193 – 218.

[28]. Seiner, J. M., Ponton, M. K., Jansen, B. J. & Lagen, N. T. 1992. The effects of temperature on supersonic jet noise emission. *DGLR/AIAA* Paper 92-02-046. Cited in Viswanathan (2004).

[29]. Doty, M. J. & McLaughlin, D. K., 2005, Space-time correlation measurements of high-speed axisymmetric jets using optical deflectometry, Experiments in Fluids, **38**, 415-425.

[30]. Seasholtz, R. G., Panda, J. & Elam, K. A. 2002. Rayleigh scattering diagnostic for measurement of velocity and density fluctuation spectra. AIAA 2002-0827.

[31]. Lee, S. S. & Bridges, J. 2005. Phased-array measurements of single flow hot jets. AIAA 2005-2842.

[32]. Bridges, J. 2006. Effect of heat on space-time correlations in jets. AIAA 2006-2534.

[33]. Mielke, A. F., Seasholtz, R. G., Elam, K. A. & Panda, J. 2005. Time-average measurement of velocity, density, temperature and turbulence velocity fluctuations using Rayleigh and Mie scattering. *Exps. Fluids* **39**, 441 – 454.

[34]. Bhat, T. R. S. 2007. Reynolds number and temperature effects on jet noise. AIAA 2007-3630.

[35]. Bridges, J. & Wernet, M. P. 2007. Effect of temperature on jet velocity spectra. AIAA 2007-3628.

[36]. Greska, B. & Krothapalli, A. 2007. A comparative study of heated single and equivalent twin jets. AIAA 2007-3634.

[37]. Wernet, M. P. 2007. Temporally resolved PIV for space-time correlations in both cold and hot jet flows. *Meas. Sci. Technol.* **18**, 1387 – 1403.

[38]. Viswanathan, K. & Czech, M. J. 2008. Role of temperature in correlating jet noise. *AIAA Journal*. Cited in Viswanathan (2009).

[39]. Harper-Bourne, M. 2009. Jet mixing noise and the effect of temperature. AIAA 2009-3255.

[40]. Mielke, A. F. & Elam, K. A. 2009a. Dynamic measurement of temperature, velocity and density in hot jets using Rayleigh scattering. *Exps. Fluids* **47**, 673 – 688.

[41]. Mielke, A. F., Elam, K. A. & Sung, C-J. 2009b. Multiproperty measurements at high sampling rates using Rayleigh scattering. *AIAA Journal* **47**, No. 4, 850 – 862.

[42]. Slot, H. J., Moore, P., Delfos, R., Bendiks, J. B. 2009. Experiments on the flow field and acoustic properties of a Mach number 0.75 turbulent air jet at a low Reynolds number. *Flow Turbulence Combust.* **83**, 587 – 611.

[43]. Karabasov, S. K., Afsar, M. Z., Hynes, T. P., Dowling, A. P., McMullen, W. A., Pokora, C. D., Page, G. J. & McGuirk, J. J. 2008. Using large eddy simulation within an acoustic analogy approach for jet noise modeling. AIAA Paper, 2008-2985.

[44]. Viswanathan, K. 2003. Jet aeroacoustic testing: issues and implications. *AIAA Journal* **41**, No. 9, 1674 – 1689.

[45]. Viswanathan, K. 2006. Scaling laws and a method for prediction of noise from single jets. . *AIAA Journal* **44**, No. 10, 2274 – 2285.

[46]. Bogey, C. & Bailly, C. 2007. An analysis of the correlations between the turbulent flow and the sound pressure fields of subsonic jets. *J. Fluid Mech.* **583**, 71 – 97.

[47]. Bogey, C., Barré, S., Juvé, D. & Bailly, C., 2009, Simulation of a hot coaxial jet: direct noise prediction and flow-acoustics correlations, Phys. Fluid, **21**, 035105, 1-14.

[48]. Gerolymos, G. A., Senechal, D. & Vallet, I. 2007. Pressure, density and temperature fluctuations in compressible turbulent flow – I. AIAA 2007-3408.

[49]. Lew, P-T., Blaisdell, G. A., Lyrintzis, A. S. 2007. Investigation of noise sources in turbulent hot jets using large eddy simulation data. AIAA 2007-16.

[50]. Bodony, D. J. 2009. Heating effects on the structure of noise sources of high-speed jets. AIAA 2009-291.

[51]. Lilley, G. M. 1996. The sound radiated from isotropic turbulence with application to the theory of jet noise. *J. Sound Vib.* **190**, No. 3, 463 – 476.

[52]. Morfey, C. L., Szewczyk, V. M. & Tester, B. J. 1978. New scaling laws for hot and cold jet mixing noise based on a geometric acoustics model. *J. Sound Vib.* **61**, 255 – 292.

[53]. Pokora, C. D., and McGuirk, J. J. 2008. Spatio-temporal turbulence correlation using a high speed PIV in an axi-symmetric jet. *AIAA Paper*, 3028-687.

[54]. Harper-Bourne, M. 2003. Jet noise measurements. AIAA 2003-3214.

[55]. Batchelor, G. K. 1953. *The theory of homogeneous turbulence*. Cambridge University Press

[56]. Khavaran, A. & Kenzakowski, D. C. 2007. Noise predictions in hot jets. AIAA 2007-3640.

[57]. Press *et al.* 1996. Numerical recipes in Fortran 77. Cambridge University Press.

[58]. Khavaran, A. 2008. Private communication.

[59]. Goldstein, M. E. 1982. High frequency sound emission from moving point mutlipole sources embedded in arbitrary transversely sheared mean flows. *J. Sound & Vib.* **80**, 499 – 521.